Electronic Supplementary Material (ESI) for Journal of Materials Chemistry A.

Supporting Information

Iodine doped composite with biomass carbon dots and reduced graphene oxide: A versatile bifunctional electrode for energy storage and oxygen reduction reaction

Van Chinh Hoang[1], Khang Ngoc Dinh[1,2], Vincent G. Gomes[1*]

[1]The University of Sydney, School of Chemical and Biomolecular Engineering, NSW 2006, Australia

[2]Energy Research Institute @ NTU (ERI@N), Interdisciplinary Graduate School, Nanyang Technological University, Singapore 637553, Singapore

* E-mail: vincent.gomes@sydney.edu.au

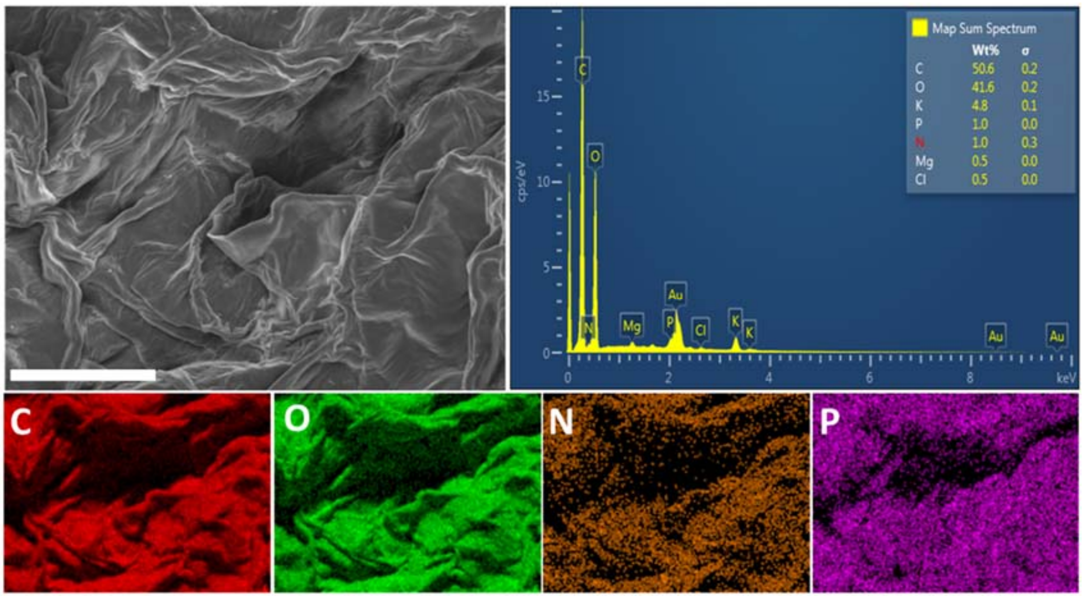

Fig S1. SEM image, EDX spectra and elemental mappings of eggplant used in this study. The scale bar is 50 µm.

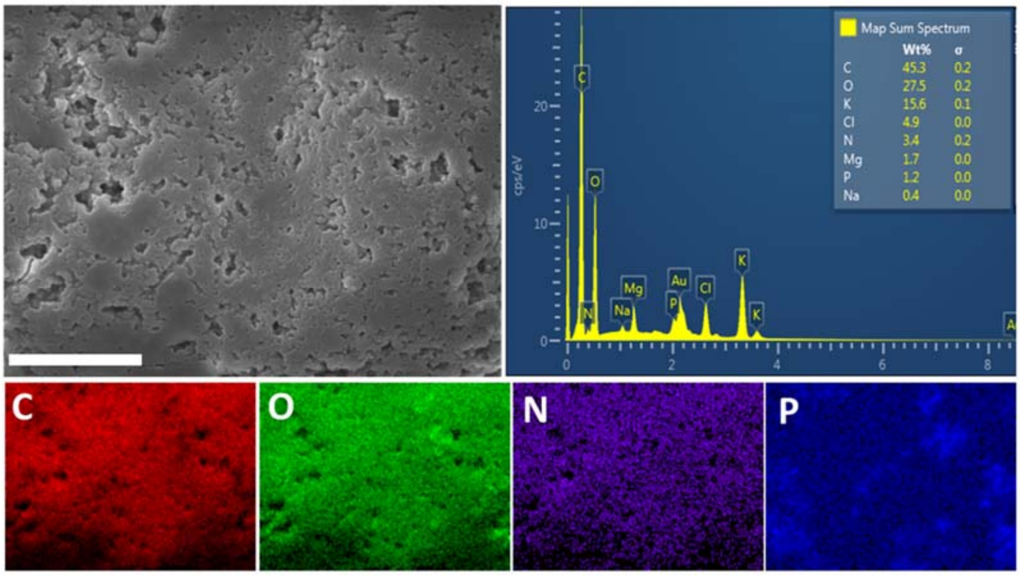

Fig S2. SEM micrograph, corresponding EDX spectrum and elemental mappings of the as-prepared CDs. The scale bar is 10 µm.

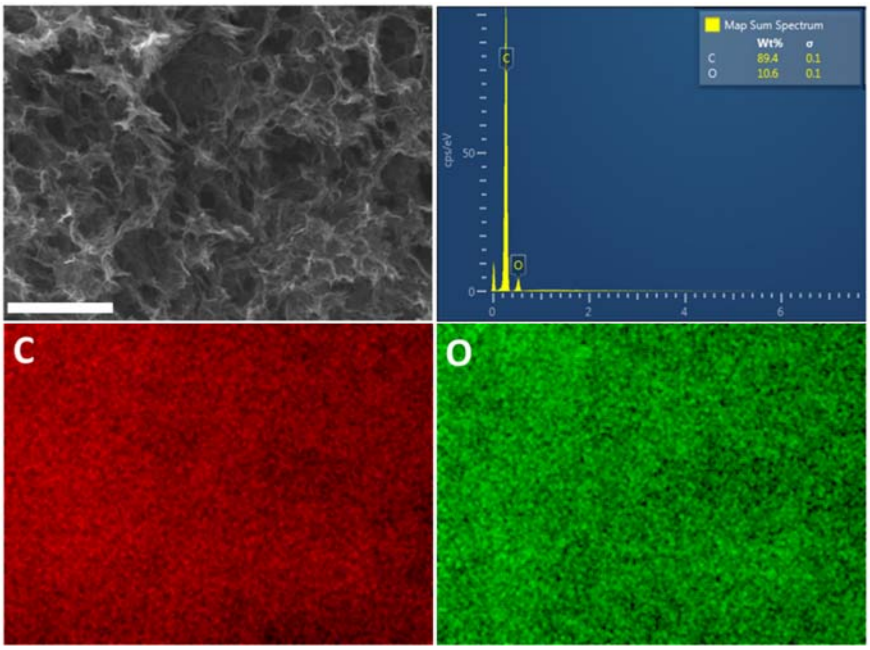

Fig S3. SEM image and corresponding EDX elemental mappings of RGO. The scale bar is 2.5 µm.

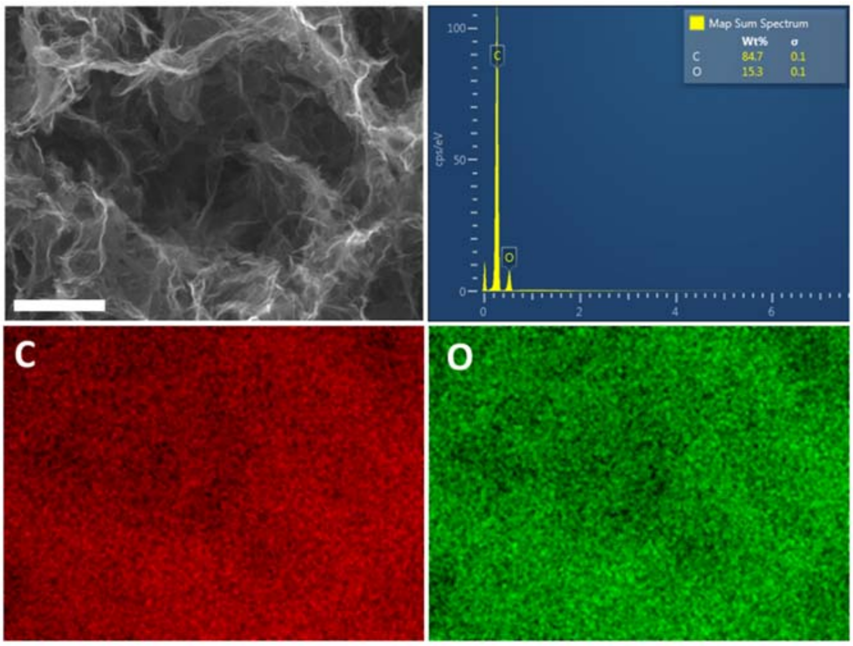

Fig S4. SEM image and corresponding EDX elemental mappings of the RGO/CDs composite. The scale bar is 2.5 μm.

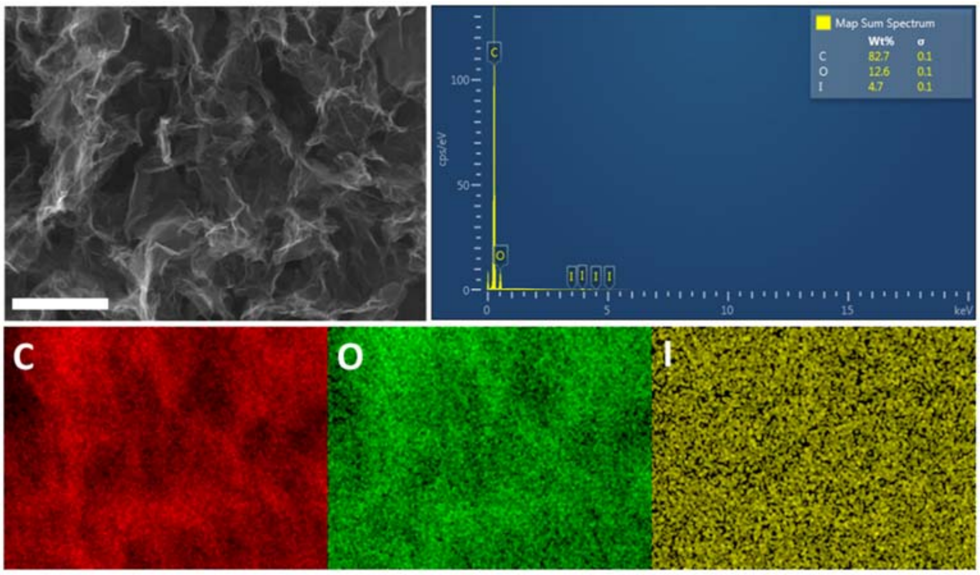

Fig S5. SEM image and corresponding EDX elemental mappings of the HI-RGO/CDs. The scale bar is 2.5 μm.

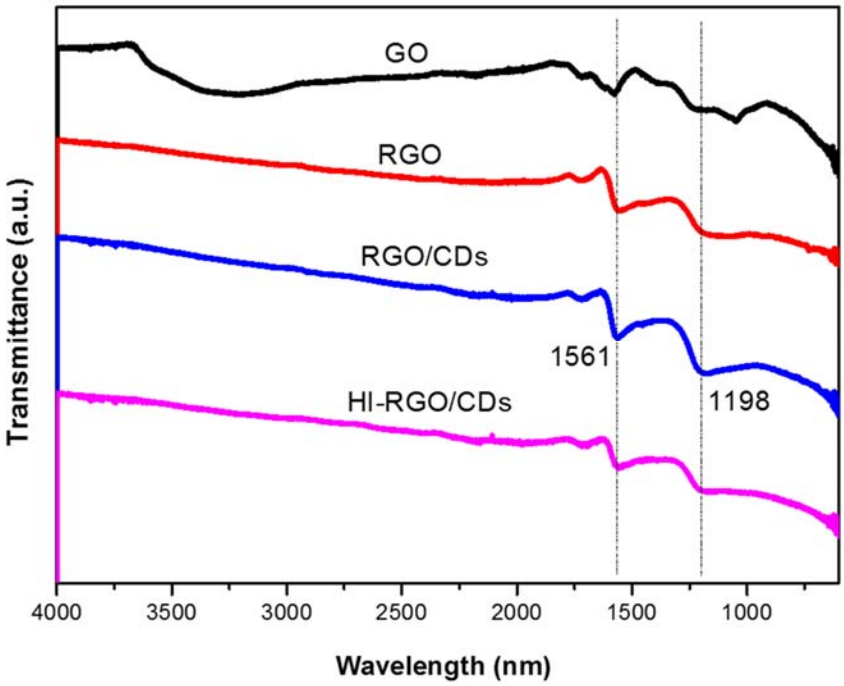

Fig S6. FTIR spectra of various samples.

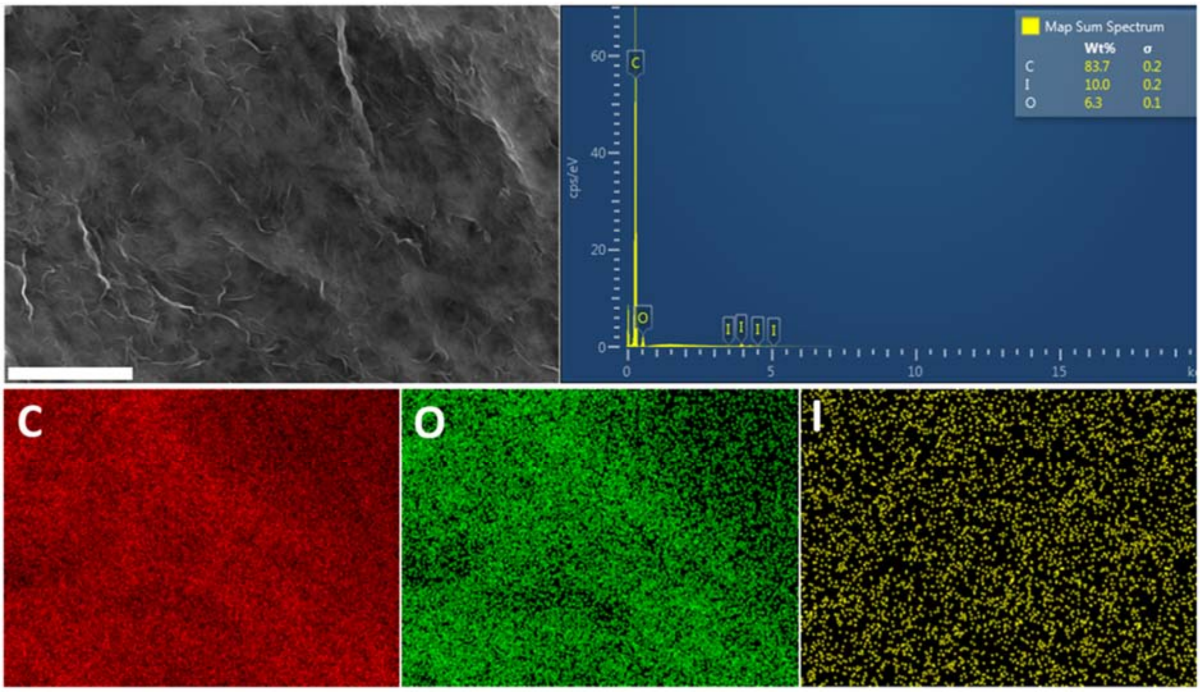

Fig S7. SEM image and corresponding EDX elemental mappings of the HI-RGO. The scale bar is 2.5 μm.

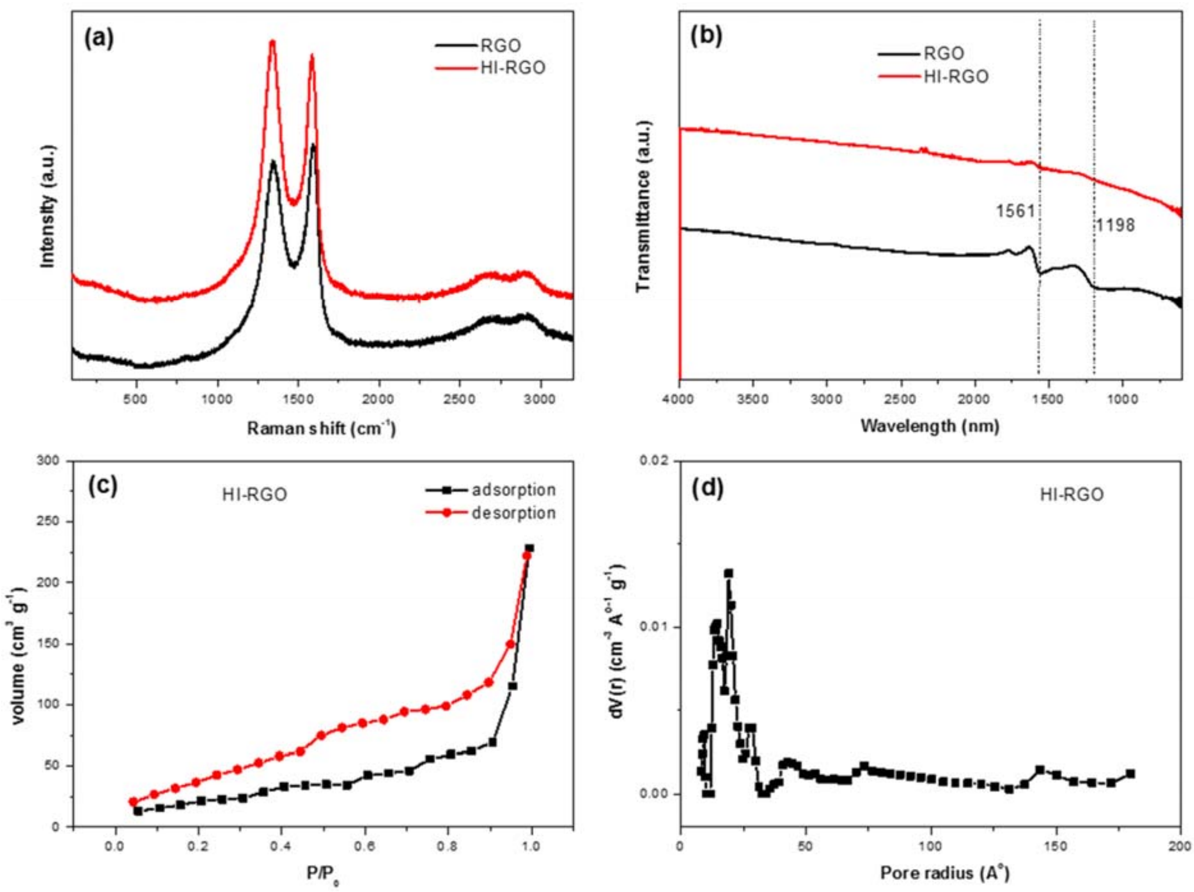

Fig S8. Comparison of Raman (a) and FTIR (b) spectra of RGO and HI-RGO, (c) nitrogen adsorption/desorption isotherms and (d) pore size distributions of HI-RGO.

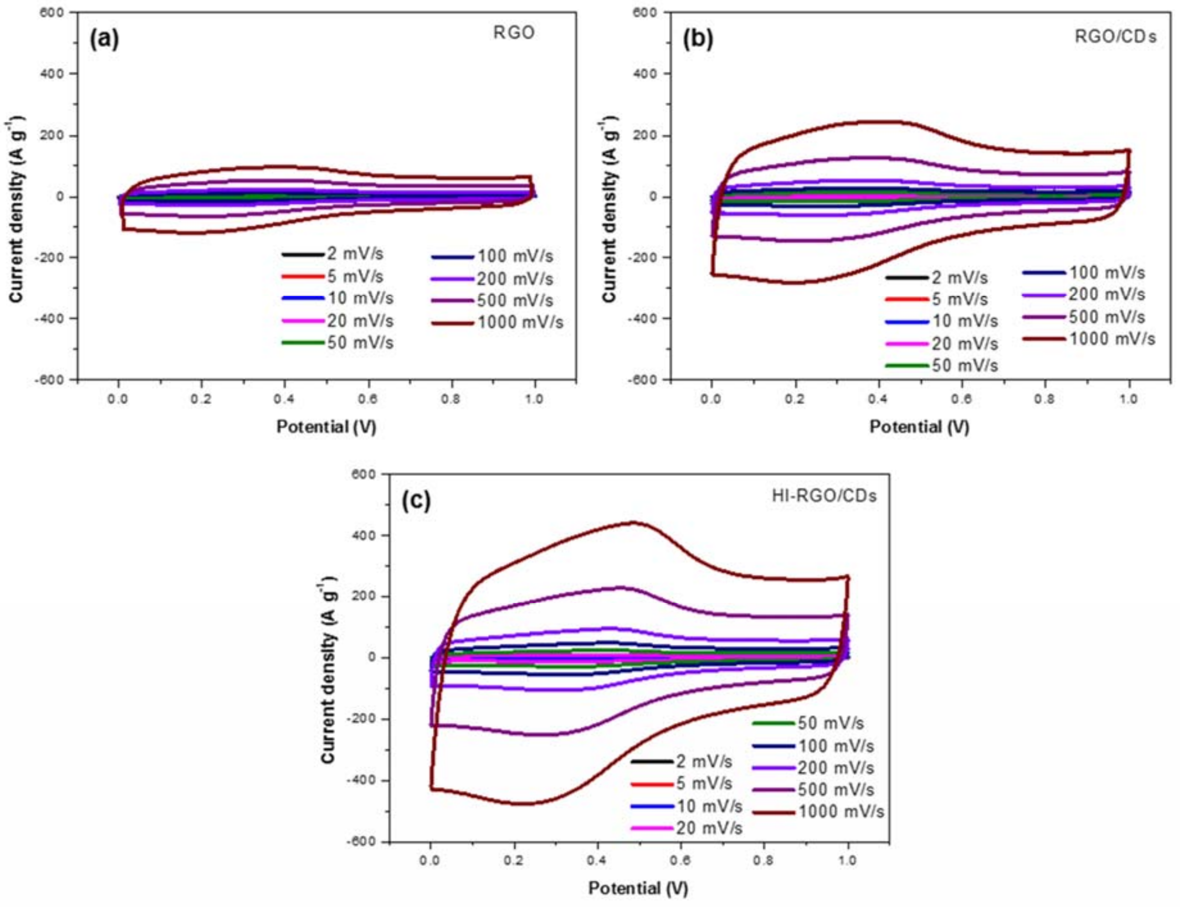

Fig S9. CV curves of (a) RGO, (b) RGO/CDs and (c) HI- RGO/CDs in 1 M H_2SO_4.

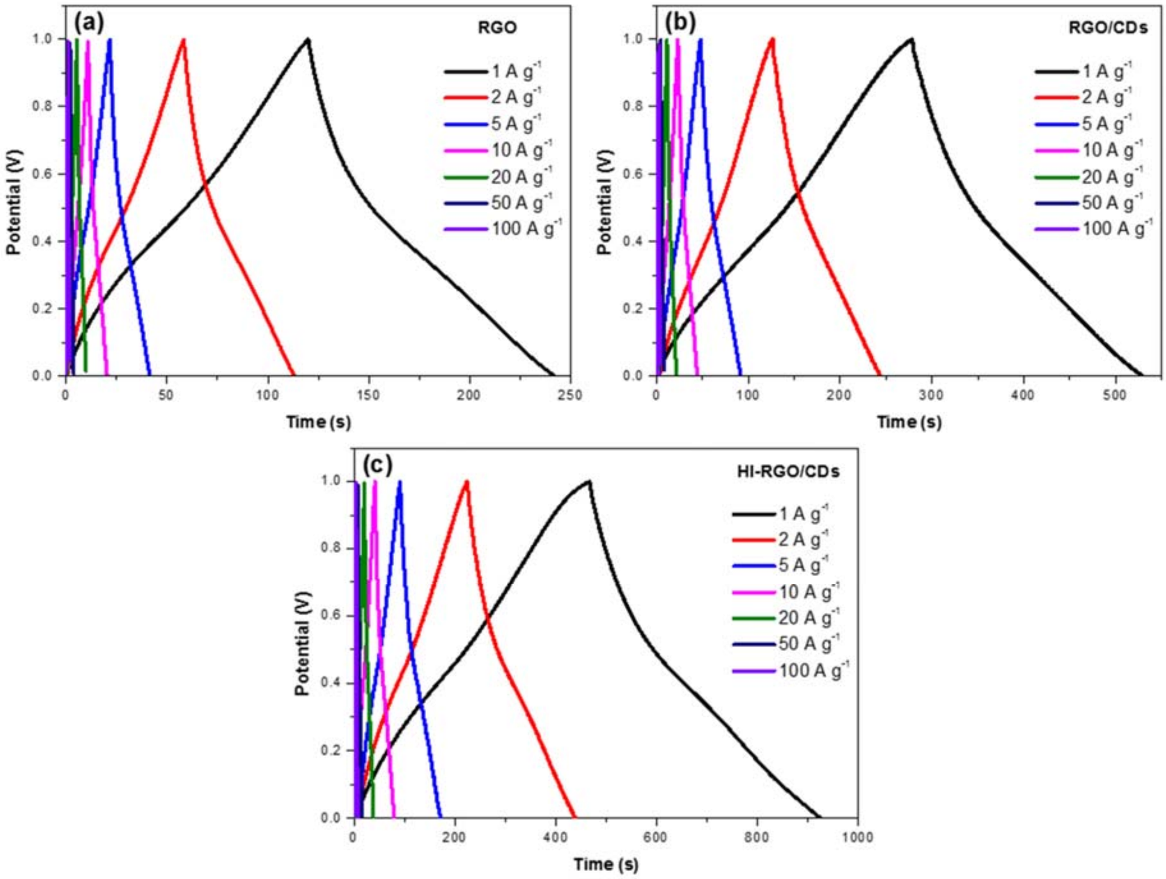

Fig S10. Galvanostatic charge/discharge curves of (a) RGO, (b) RGO/CDs and (c) HI-RGO/CDs in 1 M H_2SO_4.

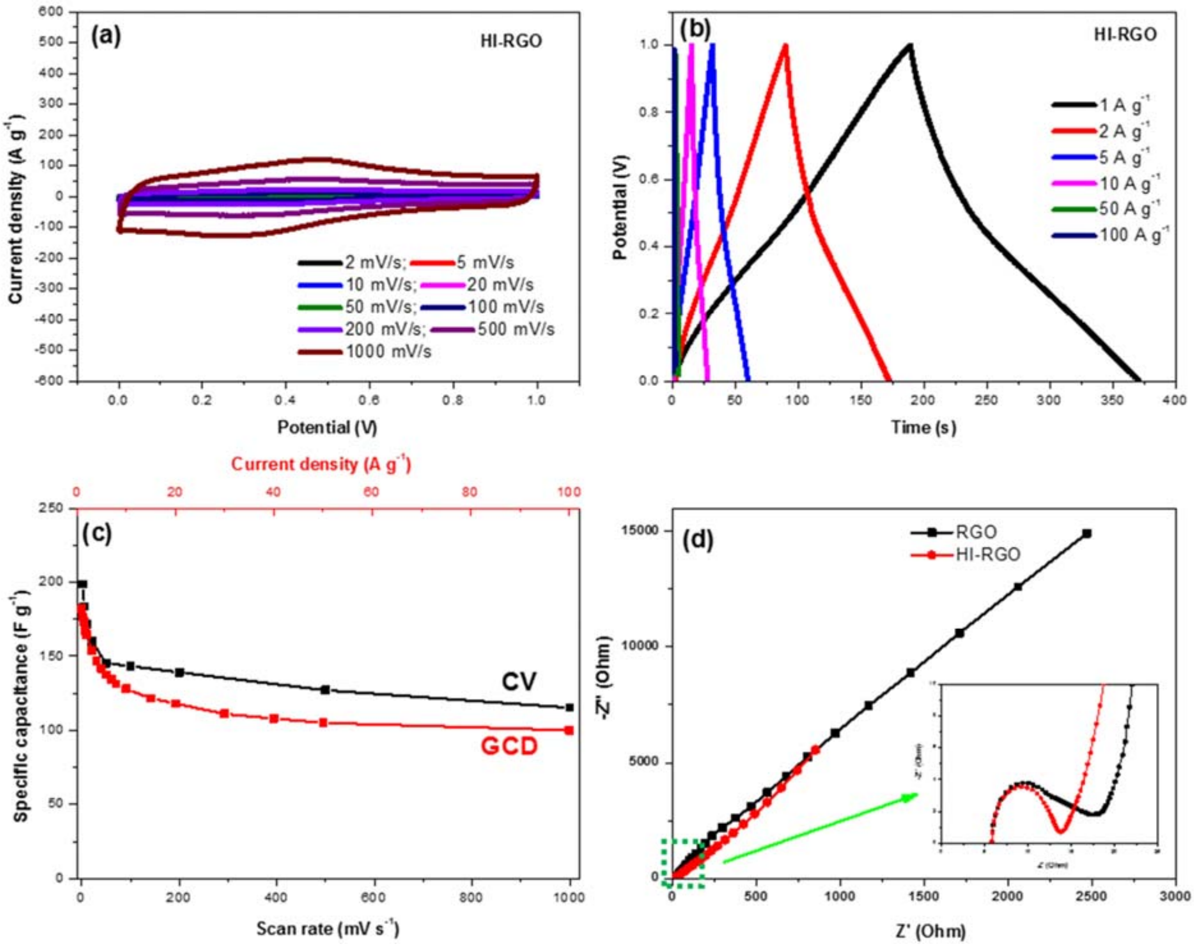

Fig S11. (a) CV curves, (b) GCD curves of HI-RGO in 1 M H_2SO_4, (c) specific capacitance of materials calculated from its CV and GCD curves, (d) comparison of Nyquist plots of RGO and HI-RGO.

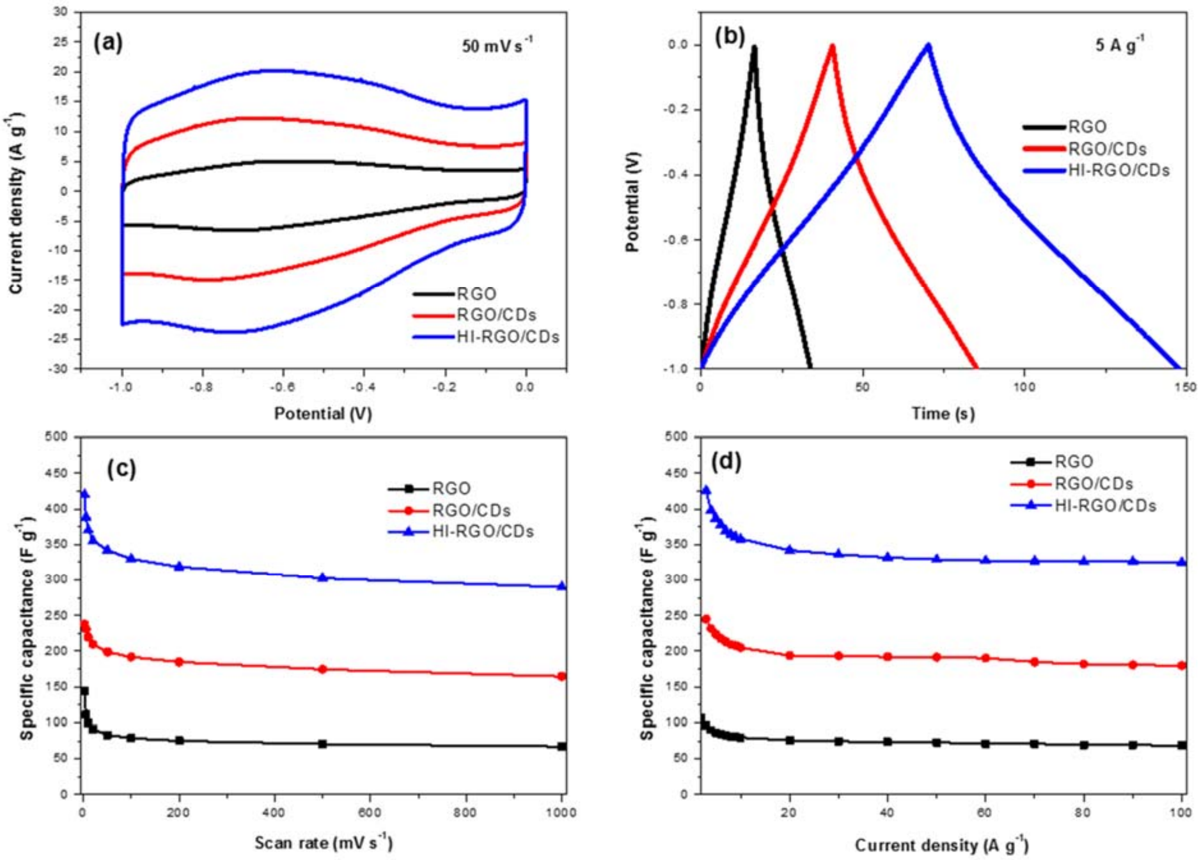

Fig S12. (a) CV curves at 50 mV s^{-1} in 1 M KOH; (b) galvanostatic charge/discharge curves at 1 A g^{-1} of three samples in 1 M KOH; (c) specific capacitances calculated from CV, (d) specific capacitances from GCD curves.

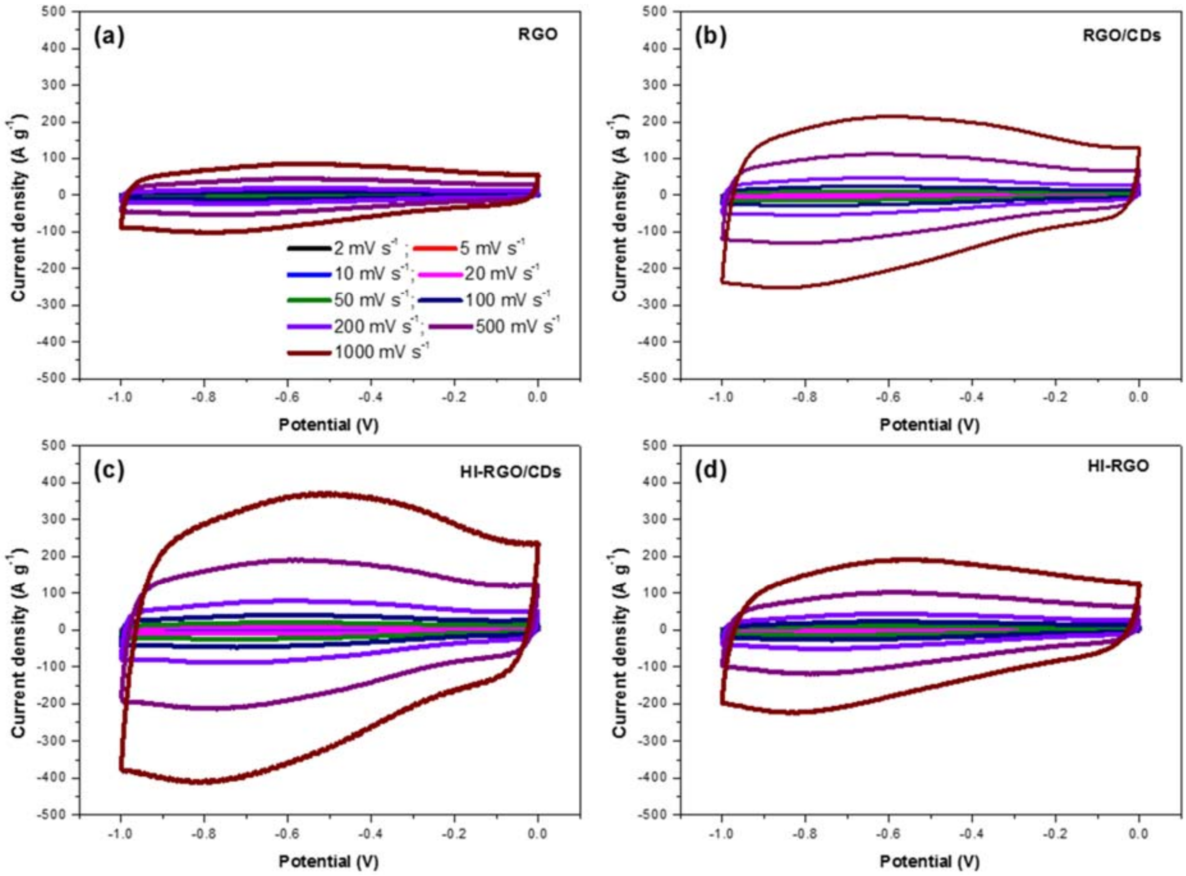

Fig S13. CV curves of (a) RGO, (b) RGO/CDs, (c) HI- RGO/CDs and (d) HI-RGO in 1 M KOH.

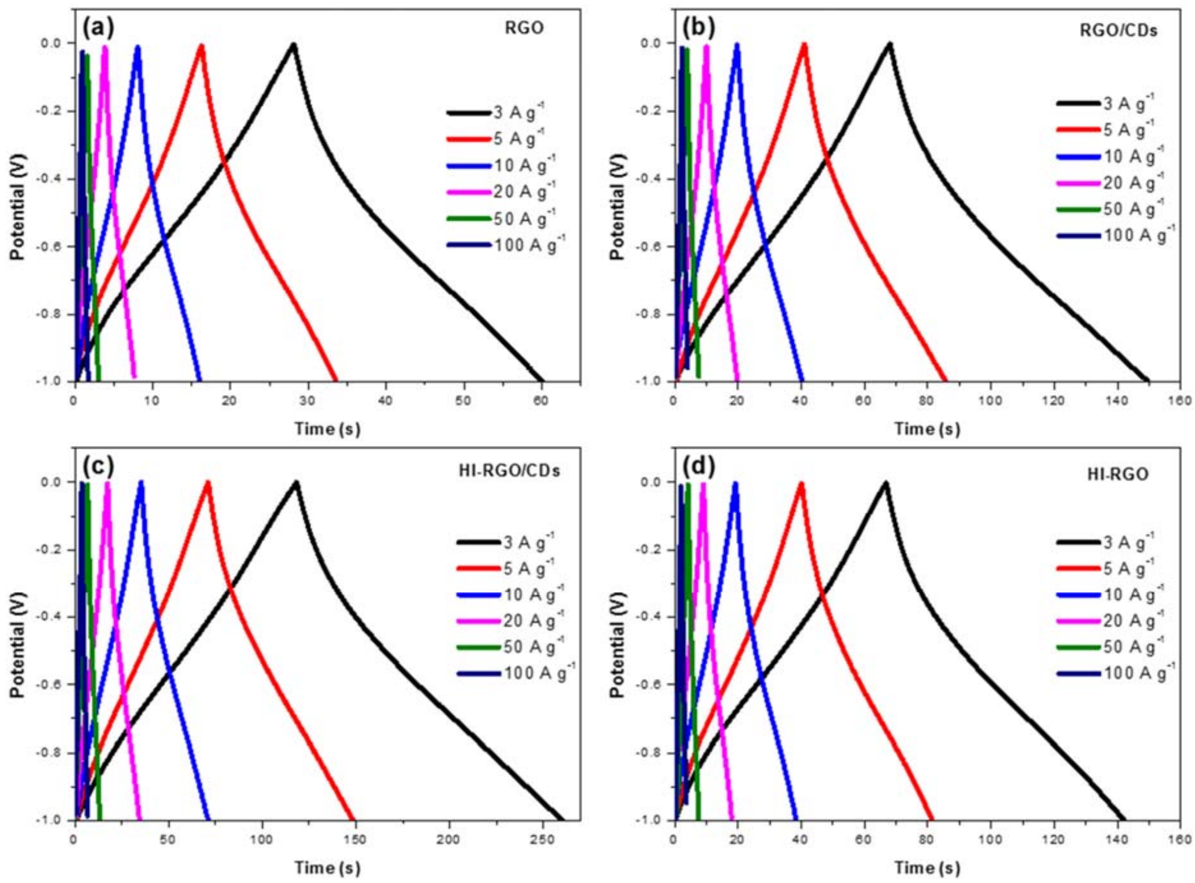

Fig S14. Galvanostatic charge/discharge curves of (a) RGO, (b) RGO/CDs, (c) HI-RGO/CDs and (d) HI-RGO in 1 M KOH.

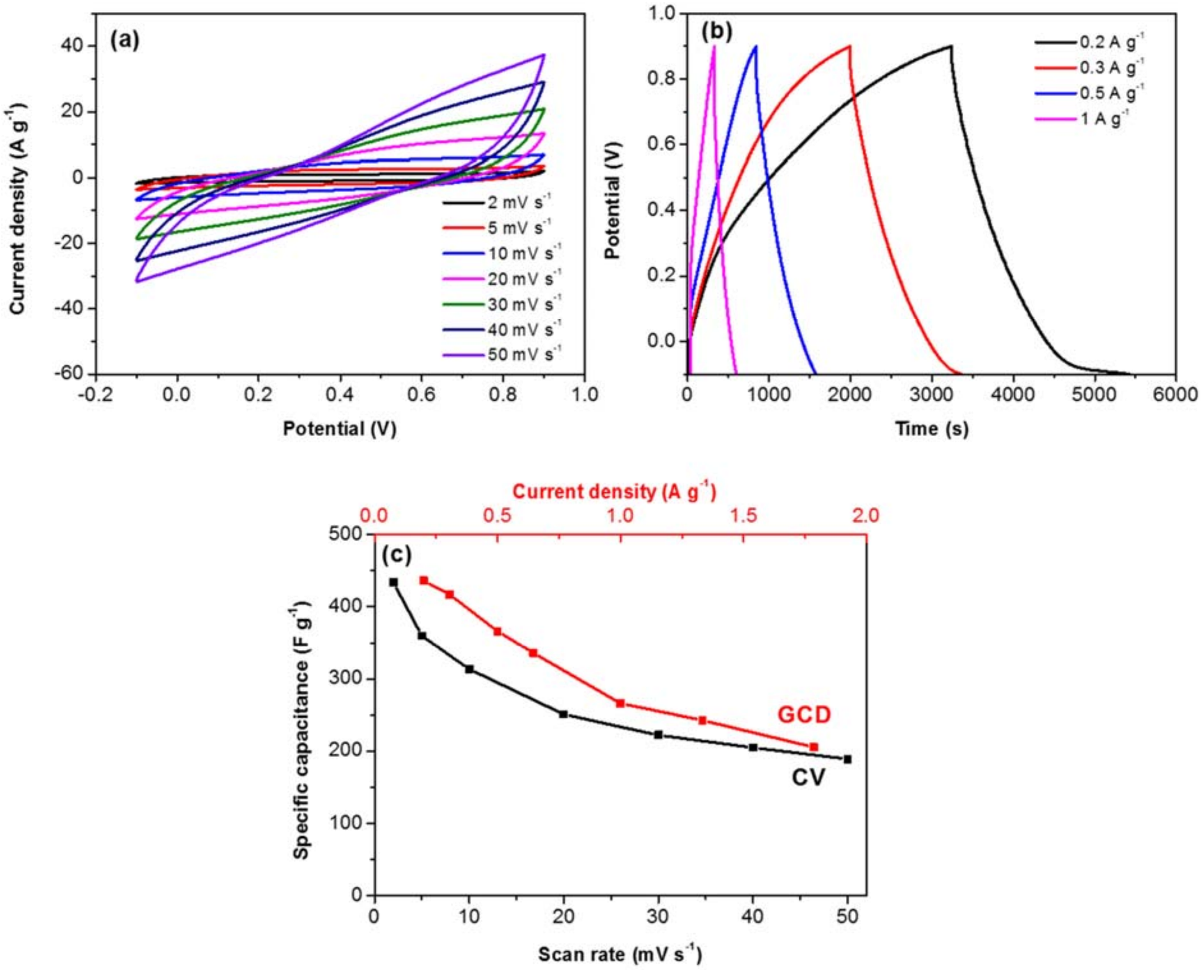

Fig S15. (a) CV curves, (b) GCD curves of HI-RGO/CDs at high loading of 8 mg cm^{-2} on Ni foam in 1 M Na_2SO_4, (c) specific capacitance of materials calculated from its CV and GCD curves.

Table S1. Comparison of graphene based supercapacitors reported in the literature.

References	**Electrode materials**	**Max specific capacitance (F g^{-1})**	**Current density / scan rate**	**Electrolyte**
This work	HI-RGO/CDs	432 295 460	2 mV s^{-1} 1,000 mV s^{-1} 1 A g^{-1}	1 M H_2SO_4

		352	100 A g^{-1}	
		420 290 426 325	2 mV s^{-1} 1,000 mV s^{-1} 3 A g^{-1} 100 A g^{-1}	1 M KOH
1	I-graphene/CDs	374 352	2 mV s^{-1} 5 mV s^{-1}	1 M KOH
2	CDs/graphene hydrogel	264 210	1 A g^{-1} 10 A g^{-1}	1 M H_2SO_4-PVA
3	N,S-codoped CDs/RGO	141	0.13 A g^{-1}	1 M Na_2SO_4
4	RGO/CDs	262 247 236	2 A g^{-1} 5 A g^{-1} 10 A g^{-1}	6 M KOH
5	CDs/RGO	212	0.5 A g^{-1}	1 M H_2SO_4
6	N-doped CDs/RGO	278 227	0.2 A g^{-1} 2 mV s^{-1}	1 M H_2SO_4
7	Graphene hydrogel	175	10 mV s^{-1}	5 M KOH
8	N,B-codoped graphene	239	1 mV s^{-1}	1 M H_2SO_4
9	Graphene/carbon aerogel	122	0.05 A g^{-1}	6 M KOH
10	N-doped graphene	282	0.2 A g^{-1}	6 M KOH
11	Graphene/SWCNT	199	0.5 A g^{-1}	EMIM-BF_4
12	Mesoporous carbon/graphene aerogel	226	1 mV s^{-1}	1 M H_2SO_4
13	Nitrogen-Superdoped 3D Graphene	380 312	0.6 A g^{-1} 5 mV s^{-1}	6 M KOH

14	Hydroquinone functionalized graphene hydrogel	441 352	1 A g^{-1} 20 A g^{-1}	1 M H_2SO_4
15	Nitrogen-doped graphene hydrogels	308	3 A g^{-1}	6 M KOH
16	Rumpled N-doped rGO sheets	479 423	1 A g^{-1} 5 mV s^{-1}	1 M H_2SO_4
17	Holey RGO framework	310	1 A g^{-1}	6 M KOH
18	Three-dimensional Nitrogen-doped graphene	334	0.5 A g^{-1}	6 M KOH
19	P-doped graphene	367	5 mV s^{-1}	1 M H_2SO_4
20	Nitrogen-doped graphene hollow nanospheres	381	1 A g^{-1}	6 M KOH
21	N doped graphene	326	0.2 A g^{-1}	6 M KOH
22	N-doped, ultralight graphene framework	484 417	1 A g^{-1} 100 A g^{-1}	1 M $LiClO_4$
23	Nitrogen doped RGO	364.6	10 mV s^{-1}	1 M H_2SO_4
24	Nitrogen doped RGO	459	1 mA cm^{-2}	1 M H_2SO_4
25	Nitrogen doped graphene	324	0.1 A g^{-1}	6 M KOH
26	Nitrogen doped RGO	340	0.5 A g^{-1}	6 M KOH
27	N-graphene from silk cocoon	348	5 mV s^{-1}	1 M H_2SO_4
28	B doped graphene	281	1 A g^{-1}	2 M H_2SO_4
29	S doped RGO	343	0.2 A g^{-1}	2 M KOH
30	S-doped RGO aerogels	445.6	5 mV s^{-1}	1 M H_2SO_4
31	N-doped RGO aerogel	350	1 A g^{-1}	1 M H_2SO_4

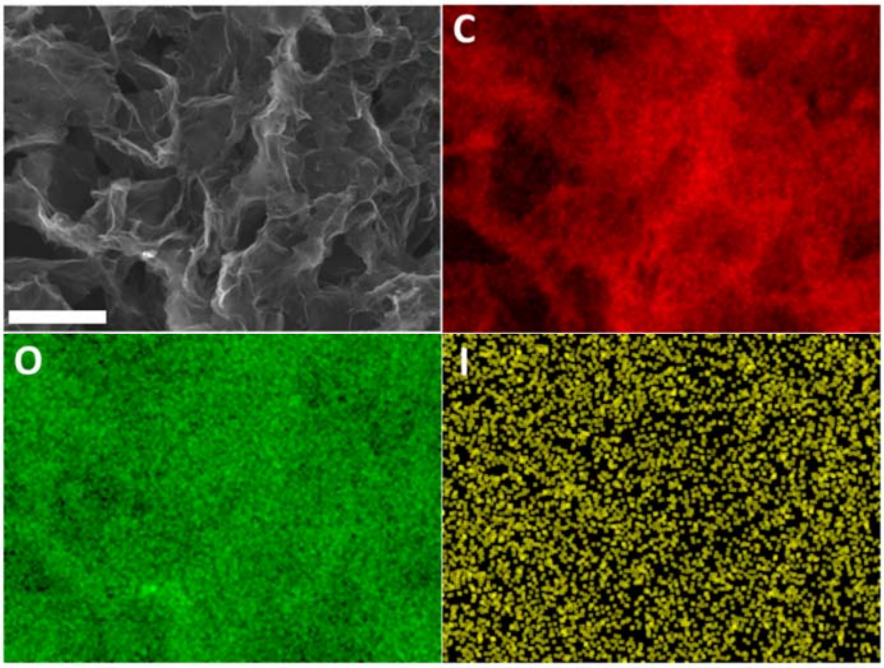

Fig S16. SEM image and corresponding EDX elemental mappings of the HI-RGO/CDs after 10,000 GCD cycles at 10 A g^{-1}. The scale bar is 2.5 μm.

Table S2. R_{ct} values, Warburg prefactor and diffusion coefficient of H^+ (D_{H+}) of HI-RGO and HI-RGO/CD electrodes.

	HI-RGO	**HI-RGO/CDs**
R_{ct} (Ω)	7.9	2.3
σ_w (Ω $s^{-1/2}$)	269.9	103.7
D_{H+} (x 10^{-18} cm^2 s^{-1})	12.6	85.5

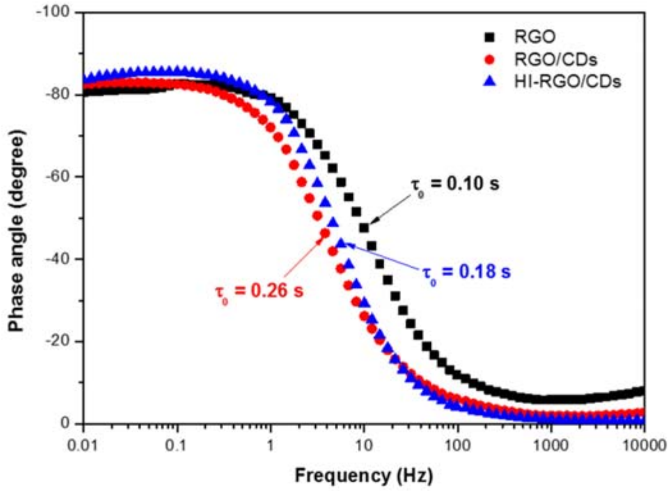

Fig S17. Bode plots of phase angle versus frequency.

Table S3. Total specific capacitance C_{sp}, electrical double layer capacitance (EDLC) and pseudo-capacitance (PC) of electrodes at scan rates, unit F g^{-1}.

Scan rate, mV s^{-1}	**RGO**			**RGO/CDs**			**HI-RGO/CDs**		
	C_{sp}	**EDLC**	**PC**	**C_{sp}**	**EDLC**	**PC**	**C_{sp}**	**EDLC**	**PC**
2	139.3	84.9	54.5	248.4	193.0	55.4	431.9	337.5	94.4
5	114.5	80.1	34.4	234.7	199.6	35.1	409.3	349.5	59.8
10	107.8	83.5	24.3	225.2	200.5	24.7	393.4	351.2	42.2
20	101.2	84.0	17.2	216.9	199.4	17.5	378.9	349.1	29.8
50	95.2	84.3	10.9	206.4	195.3	11.1	360.8	342.0	18.8
100	90.9	83.2	7.7	199.5	191.7	7.8	348.4	335.0	13.4
200	84.3	78.8	5.5	192.7	187.2	5.5	335.5	326.1	9.4
500	77.8	74.3	3.5	182.8	179.3	3.5	315.5	309.5	6.0
1000	70.5	68.1	2.4	173.8	171.3	2.5	295.3	291.1	4.2

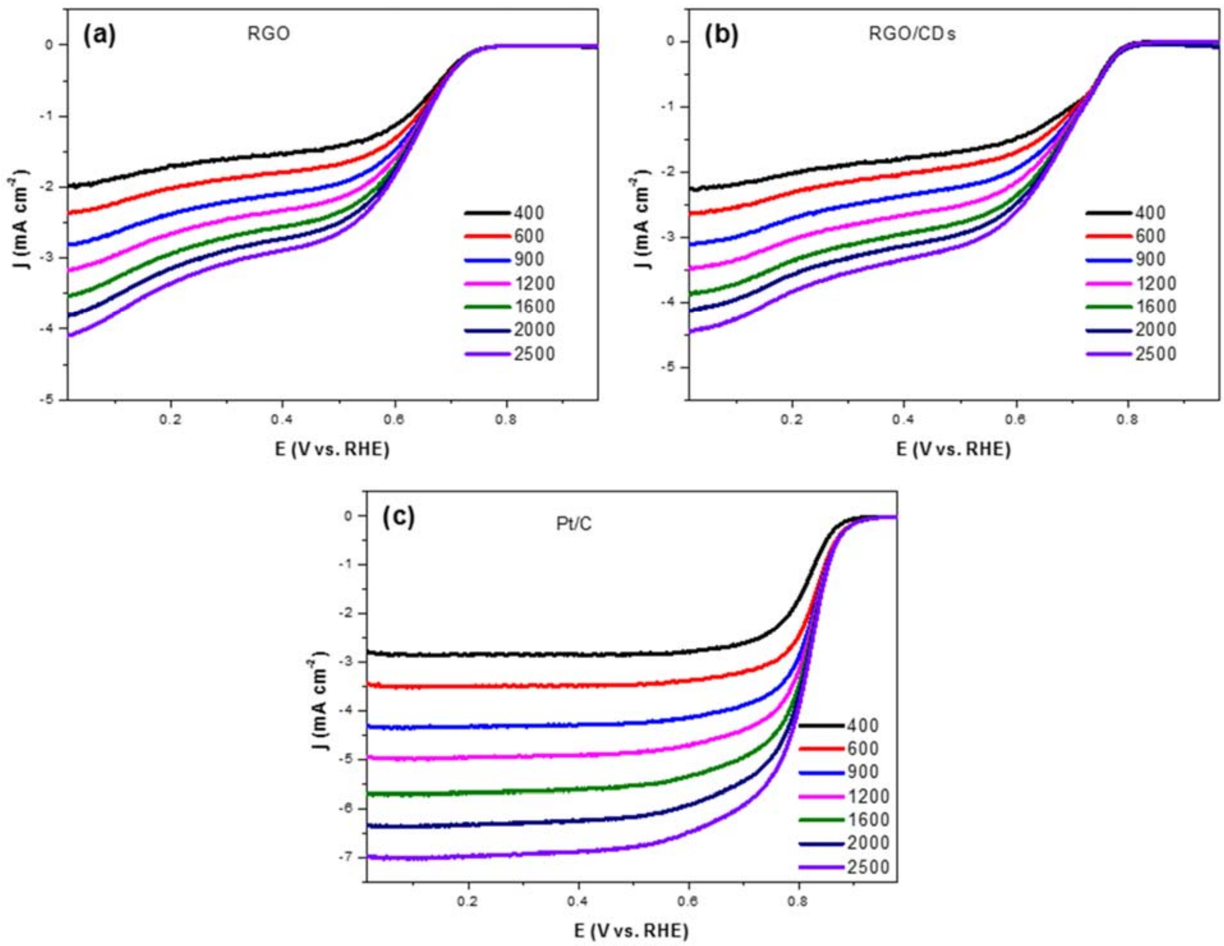

Fig S18. LSV curves of (a) RGO, (b) RGO/CDs and (c) Pt/C at various rotation frequencies in O_2-saturated 0.1 M KOH.

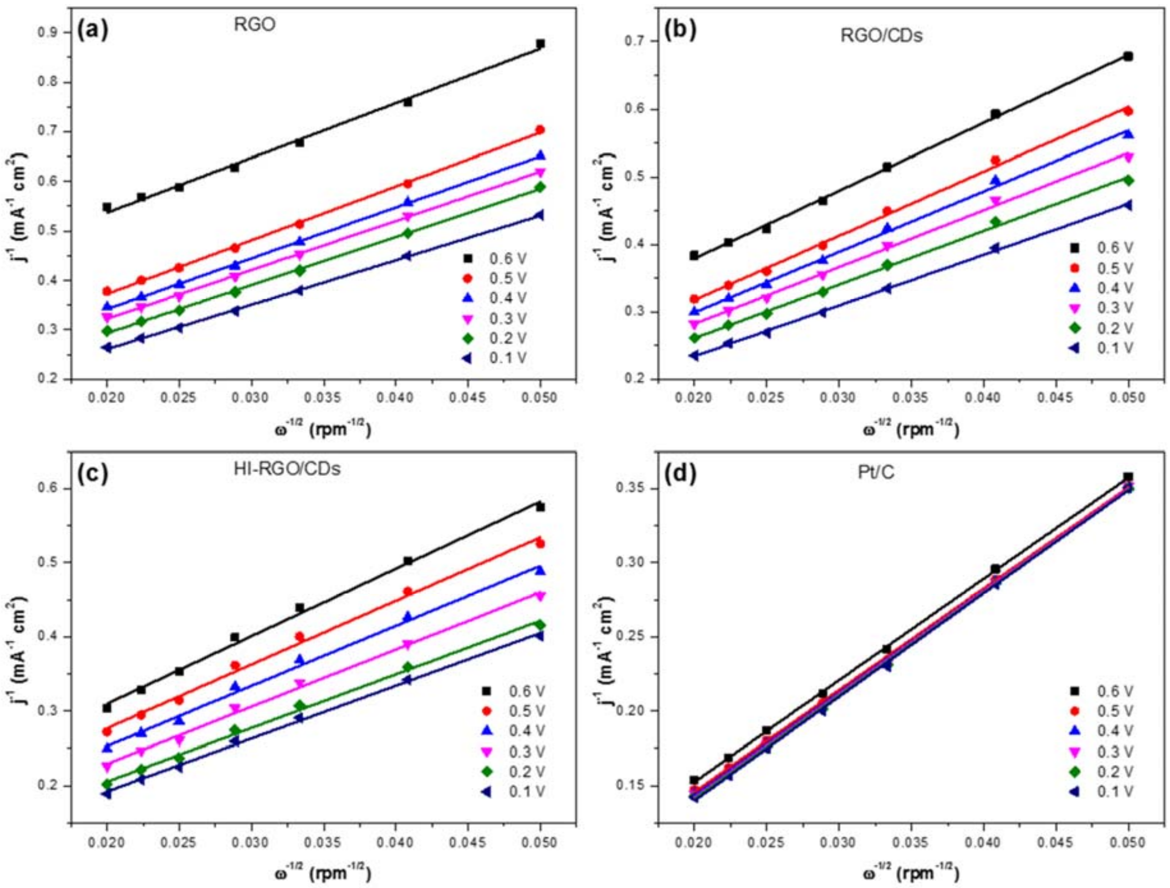

Fig S19. Koutecky–Levich plots of (a) RGO, (b) RGO/CDs, (c) HI-RGO/CDs and (d) Pt/C at several potentials in O_2-saturated 0.1 M KOH.

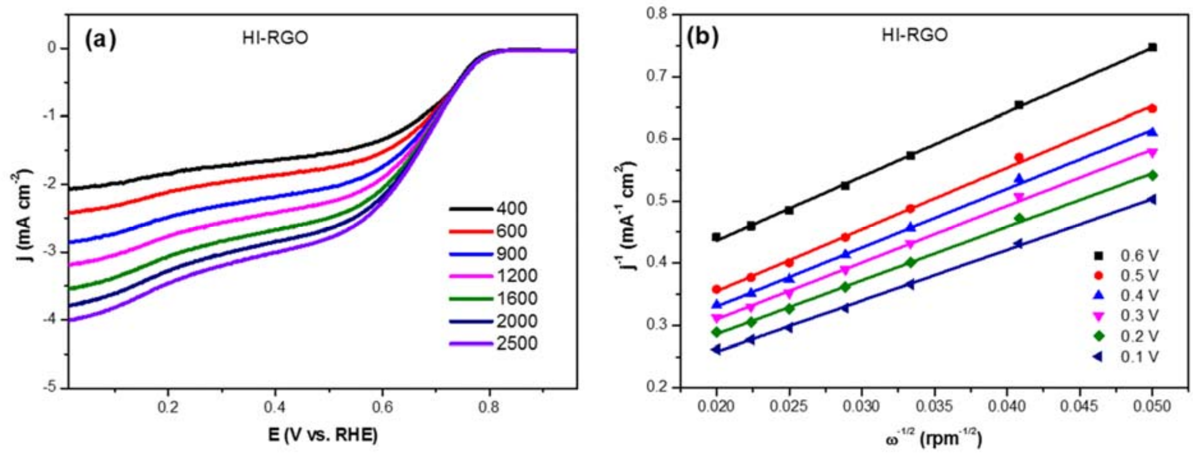

Fig S20. (a) LSV curves of HI-RGO at various rotation frequencies in O_2-saturated 0.1 M KOH. (b) Koutecky–Levich plots HI-RGO at several potentials in O_2-saturated 0.1 M KOH.

Table S4. Comparison of metal-free carbon based ORR electrocatalysts reported in the literature.

References	**Catalysts**	**Onset potential (V) vs. RHE**	**j_L (mA cm^{-2})**	**j_k (mA cm^{-2})**	**Electron transfer number, n**
This work	HI-RGO/CDs	0.93	4.62	19.8	3.1-4.0
32	Cl-graphene nanoplatelet	0.804	0.18 mA		3.5 (-0.8 V)
32	Br-graphene nanoplatelet	~ 0.814	0.28 mA		3.8 (-0.8 V)
32	I-graphene nanoplatelet	0.824	0.4 mA		3.9 (-0.8 V)
33	I-graphene	0.884	7.2	9.21	3.86
34	N,I-codoped graphene	0.884		11.76	3.93
35	B-doped graphene	0.914	~0.54 mA		3.5
36	Plasma-treated graphene	0.912			3.85
36	Graphene	0.806			2.31
37	N-graphene	0.826	2.0		1.7-2.0
37	N-CNT	0.837	2.1		1.9-2.3
37	N-graphene/N-CNT	0.869	3.2		3.3-3.7
38	N-graphene	0.764	0.8		3.6-4
39	N-graphene	0.924	~5.1		3.3-4
40	N-GQDs	0.969			3.9
41	N-graphene/CNT	0.91	~5.4		3.78-3.93
42	N-hollow mesoporous graphene analogous spheres	0.14			3.9
43	N,P-carbon	0.9	~5.0	12.9	3.86
44	N, P-mesoporous nanocarbon	0.94	~4.2	~26	3.85
45	N,P-CNTs/ graphene nanospheres	0.94		5.9	3.95
46	R2CPC	0.778			2.5
46	R4CPC	0.738			3.7
3	N,S-graphene/CDs	0.84			3.5-3.75
47	N-doped carbon aerogels	0.844			3-3.7
48	Soy protein- derived porous carbon aerogels	0.904			3.3-3.7
49	N,S-carbon aerogels	0.834			2.7-3.7
50	N-porous carbon	0.85	2.67	2.42	3.5-3.9
51	N-doped carbon	1.224	4.24		3.4
52	Cellulose-derived carbon	~ 0.92	3.3	6.9	3.6-3.9
53	Corn starch-derived carbon nanosheets	0.934	4.5	8.1	3.5
54	N-carbon fiber aerogel	1.01	4.7		3.47-3.9

55	Chitosan-derived N-carbon	0.934	4.9	37.04	3.42-3.67
56	N,S-carbon nanoplatelets	0.97	7.06		3.8
57	Water hyacinth derived porous carbon	0.98	4.5	1.04	3.51-3.82
58	Bamboo fungus derived carbon	0.089[a]	3.55		3.6
59	Pulsatilla chinensis (bunge) Regel-derived carbon	0.944	4.36		3.46-3.6
60	Human urine-derived porous carbon	0.934	3.5		3.7
61	N,S-codoped 3D porous graphene	0.904	5.34		3.52-3.83

[a] The potential is given with respect to Hg/HgO reference electrode.

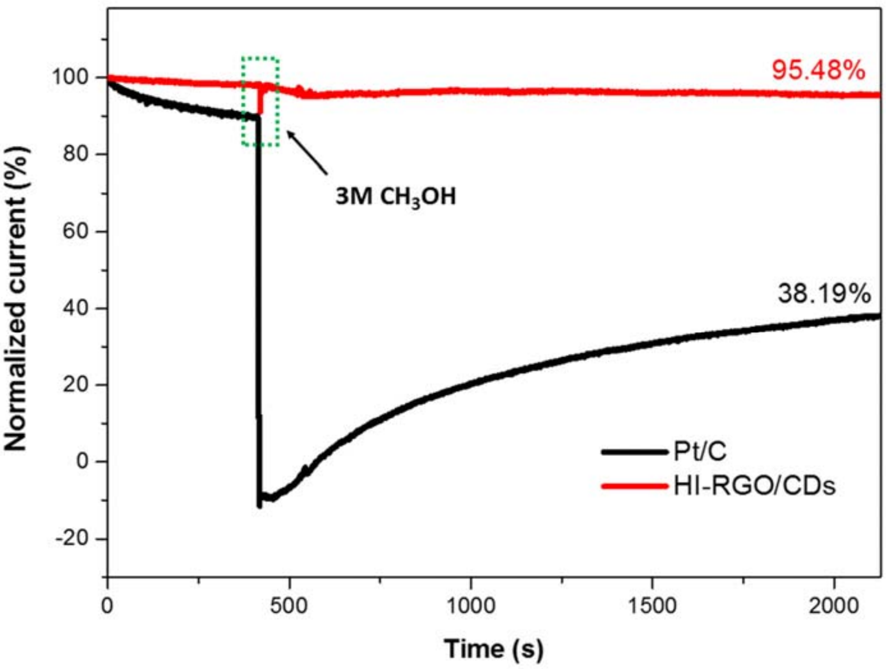

Fig S21. i-t chronoamperometric reponses of HI-RGO/CDs and commercial Pt/C before and after the addition of 3.0 M methanol to O_2-saturated 0.1 M KOH electrolytes.

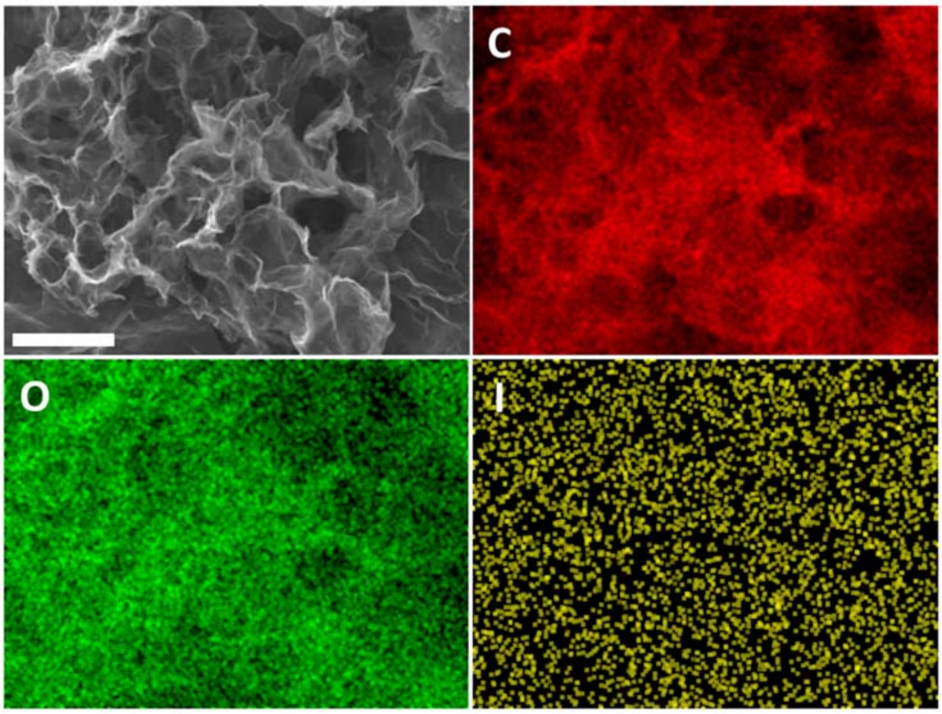

Fig S22. SEM image and corresponding EDX elemental mappings of the HI-RGO/CDs after 22 h ORR stability test. The scale bar is 2.5 μm.

ECSA of materials

The electrochemically active surface areas (ECSA) of the samples were determined from their double layer capacitance (C_{dl}). CV scans were carried out in a non-Faradaic region between -0.1 and 0 V (vs. Ag/AgCl) at various scan rates from 5 to 100 mV s^{-1} in 0.1 M KOH. C_{dl} was calculated from following formula:

$$C_{dl} = \frac{1}{2V\nu}\int_{V_-}^{V_+} i(V)dV \qquad (1)$$

ECSA was then normallized by specific capacitance of corresponding materials (C_s):

$$\text{ECSA} = \frac{C_{dl}}{C_s} \qquad (2)$$

Since a commonly used C_s value for carbon is 20 mF cm^{-2} [62], we calculated ECSA values of the catalysts and the results are depicted in Fig S21e.

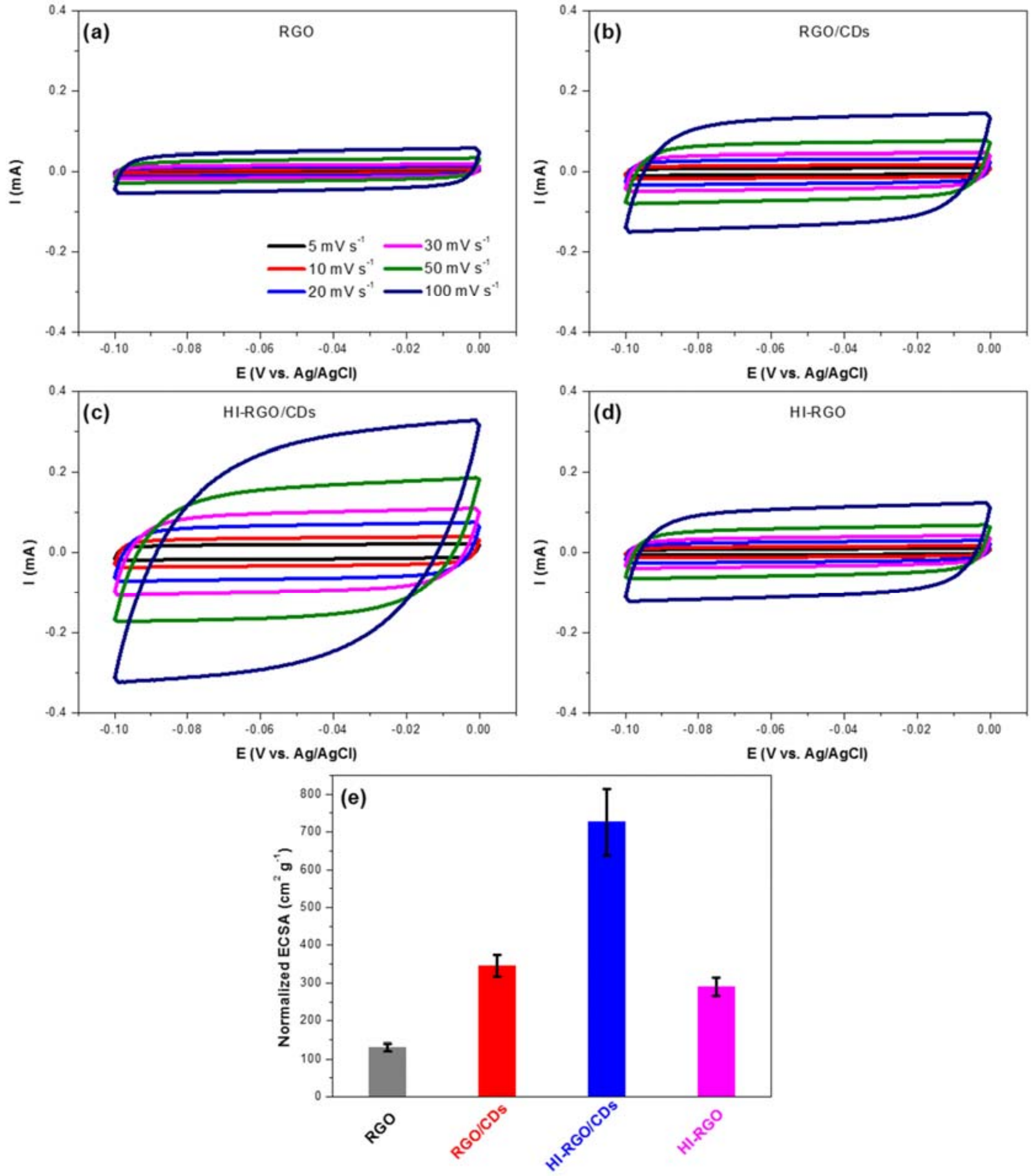

Fig S23. CV scan curves of (a) RGO, (b) RGO/CDs, (c) HI-RGO/CDs and (d) HI-RGO at variable scan rates from 5 to 100 mV s^{-1} in 0.1 M KOH; (e) corresponding ECSA of four electrodes.

References

1. V. C. Hoang and V. G. Gomes, *Materials Today Energy*, 2019, **12**, 198-207.
2. H. Feng, P. Xie, S. Xue, L. Li, X. Hou, Z. Liu, D. Wu, L. Wang and P. K. Chu, *Journal of Electroanalytical Chemistry*, 2018, **808**, 321-328.
3. A. K. Samantara, S. Chandra Sahu, A. Ghosh and B. K. Jena, *Journal of Materials Chemistry A*, 2015, **3**, 16961-16970.
4. X. Zhao, M. Li, H. Dong, Y. Liu, H. Hu, Y. Cai, Y. Liang, Y. Xiao and M. Zheng, *ChemSusChem*, 2017, **10**, 2626-2634.
5. Y. Q. Dang, S. Z. Ren, G. Liu, J. Cai, Y. Zhang and J. Qiu, *Nanomaterials (Basel)*, 2016, **6**.
6. V. C. Hoang, L. H. Nguyen and V. G. Gomes, *Journal of Electroanalytical Chemistry*, 2019, **832**, 87-96.
7. Y. Xu, K. Sheng, C. Li and G. Shi, *ACS Nano*, 2010, **4**, 4324-4330.
8. Z.-S. Wu, A. Winter, L. Chen, Y. Sun, A. Turchanin, X. Feng and K. Müllen, *Advanced Materials*, 2012, **24**, 5130-5135.
9. F. Meng, X. Zhang, B. Xu, S. Yue, H. Guo and Y. Luo, *Journal of Materials Chemistry*, 2011, **21**, 18537-18539.
10. H. M. Jeong, J. W. Lee, W. H. Shin, Y. J. Choi, H. J. Shin, J. K. Kang and J. W. Choi, *Nano Letters*, 2011, **11**, 2472-2477.
11. D. T. Pham, T. H. Lee, D. H. Luong, F. Yao, A. Ghosh, V. T. Le, T. H. Kim, B. Li, J. Chang and Y. H. Lee, *ACS Nano*, 2015, **9**, 2018-2027.
12. Z.-S. Wu, Y. Sun, Y.-Z. Tan, S. Yang, X. Feng and K. Müllen, *Journal of the American Chemical Society*, 2012, **134**, 19532-19535.
13. W. Zhang, C. Xu, C. Ma, G. Li, Y. Wang, K. Zhang, F. Li, C. Liu, H. M. Cheng, Y. Du, N. Tang and W. Ren, *Adv Mater*, 2017, **29**.
14. Y. Xu, Z. Lin, X. Huang, Y. Wang, Y. Huang and X. Duan, *Adv Mater*, 2013, **25**, 5779-5784.
15. H.-L. Guo, P. Su, X. Kang and S.-K. Ning, *J. Mater. Chem. A*, 2013, **1**, 2248-2255.
16. Y. Zhao, J. Liu, B. Wang, J. Sha, Y. Li, D. Zheng, M. Amjadipour, J. MacLeod and N. Motta, *ACS Appl Mater Interfaces*, 2017, **9**, 22588-22596.
17. Y. Xu, Z. Lin, X. Zhong, X. Huang, N. O. Weiss, Y. Huang and X. Duan, *Nat Commun*, 2014, **5**, 4554.
18. X. Zhao, H. Dong, Y. Xiao, H. Hu, Y. Cai, Y. Liang, L. Sun, Y. Liu and M. Zheng, *Electrochimica Acta*, 2016, **218**, 32-40.
19. P. Karthika, N. Rajalakshmi and K. S. Dhathathreyan, *Journal of Nanoscience and Nanotechnology*, 2013, **13**, 1746-1751.
20. W. Fan, Y.-Y. Xia, W. W. Tjiu, P. K. Pallathadka, C. He and T. Liu, *Journal of Power Sources*, 2013, **243**, 973-981.
21. L. Sun, L. Wang, C. Tian, T. Tan, Y. Xie, K. Shi, M. Li and H. Fu, *RSC Advances*, 2012, **2**, 4498-4506.
22. Y. Zhao, C. Hu, Y. Hu, H. Cheng, G. Shi and L. Qu, *Angewandte Chemie International Edition*, 2012, **51**, 11371-11375.
23. C. Chen, W. Fan, T. Ma and X. Fu, *Ionics*, 2014, **20**, 1489-1494.
24. M. P. Kumar, T. Kesavan, G. Kalita, P. Ragupathy, T. N. Narayanan and D. K. Pattanayak, *RSC Advances*, 2014, **4**, 38689-38697.

25. H. Jin, X. Wang, Z. Gu, Q. Fan and B. Luo, *Journal of Power Sources*, 2015, **273**, 1156-1162.
26. H. Luo, Z. Liu, L. Chao, X. Wu, X. Lei, Z. Chang and X. Sun, *Journal of Materials Chemistry A*, 2015, **3**, 3667-3675.
27. V. Sahu, S. Grover, B. Tulachan, M. Sharma, G. Srivastava, M. Roy, M. Saxena, N. Sethy, K. Bhargava, D. Philip, H. Kim, G. Singh, S. K. Singh, M. Das and R. K. Sharma, *Electrochimica Acta*, 2015, **160**, 244-253.
28. Z. Zuo, Z. Jiang and A. Manthiram, *Journal of Materials Chemistry A*, 2013, **1**, 13476-13483.
29. X. a. Chen, X. Chen, X. Xu, Z. Yang, Z. Liu, L. Zhang, X. Xu, Y. Chen and S. Huang, *Nanoscale*, 2014, **6**, 13740-13747.
30. X. Yu, S. K. Park, S.-H. Yeon and H. S. Park, *Journal of Power Sources*, 2015, **278**, 484-489.
31. Y. Du, L. Liu, Y. Xiang and Q. Zhang, *Journal of Power Sources*, 2018, **379**, 240-248.
32. I.-Y. Jeon, H.-J. Choi, M. Choi, J.-M. Seo, S.-M. Jung, M.-J. Kim, S. Zhang, L. Zhang, Z. Xia, L. Dai, N. Park and J.-B. Baek, *Scientific Reports*, 2013, **3**, 1810.
33. Z. Yao, H. Nie, Z. Yang, X. Zhou, Z. Liu and S. Huang, *Chemical Communications*, 2012, **48**, 1027-1029.
34. M. Hassan, E. Haque, A. I. Minett and V. G. Gomes, *ChemSusChem*, 2015, **8**, 4040-4048.
35. Z.-H. Sheng, H.-L. Gao, W.-J. Bao, F.-B. Wang and X.-H. Xia, *Journal of Materials Chemistry*, 2012, **22**, 390-395.
36. L. Tao, Q. Wang, S. Dou, Z. Ma, J. Huo, S. Wang and L. Dai, *Chemical Communications*, 2016, **52**, 2764-2767.
37. P. Chen, T.-Y. Xiao, Y.-H. Qian, S.-S. Li and S.-H. Yu, *Advanced Materials*, 2013, **25**, 3192-3196.
38. L. Qu, Y. Liu, J.-B. Baek and L. Dai, *ACS Nano*, 2010, **4**, 1321-1326.
39. C. Zhang, R. Hao, H. Liao and Y. Hou, *Nano Energy*, 2013, **2**, 88-97.
40. Q. Li, S. Zhang, L. Dai and L.-s. Li, *Journal of the American Chemical Society*, 2012, **134**, 18932-18935.
41. C. H. Choi, M. W. Chung, H. C. Kwon, J. H. Chung and S. I. Woo, *Applied Catalysis B: Environmental*, 2014, **144**, 760-766.
42. J. Yan, H. Meng, F. Xie, X. Yuan, W. Yu, W. Lin, W. Ouyang and D. Yuan, *Journal of Power Sources*, 2014, **245**, 772-778.
43. X. Chen, L. Wei, Y. Wang, S. Zhai, Z. Chen, S. Tan, Z. Zhou, A. K. Ng, X. Liao and Y. Chen, *Energy Storage Materials*, 2018, **11**, 134-143.
44. J. Zhang, Z. Zhao, Z. Xia and L. Dai, *Nature Nanotechnology*, 2015, **10**, 444.
45. J. Yang, H. Sun, H. Liang, H. Ji, L. Song, C. Gao and H. Xu, *Advanced Materials*, 2016, **28**, 4606-4613.
46. N. López-Salas, M. C. Gutiérrez, C. O. Ania, M. A. Muñoz-Márquez, M. Luisa Ferrer and F. d. Monte, *Journal of Materials Chemistry A*, 2016, **4**, 478-488.
47. N. Brun, S. A. Wohlgemuth, P. Osiceanu and M. M. Titirici, *Green Chemistry*, 2013, **15**, 2514-2524.
48. S.-M. Alatalo, K. Qiu, K. Preuss, A. Marinovic, M. Sevilla, M. Sillanpää, X. Guo and M.-M. Titirici, *Carbon*, 2016, **96**, 622-630.
49. S.-A. Wohlgemuth, R. J. White, M.-G. Willinger, M.-M. Titirici and M. Antonietti, *Green Chemistry*, 2012, **14**, 1515-1523.

50. X. Liu, L. Li, W. Zhou, Y. Zhou, W. Niu and S. Chen, *ChemElectroChem*, 2015, **2**, 803-810.
51. K. Ding, Q. Liu, Y. Bu, Y. Huang, J. Lv, J. Wu, S. C. Abbas and Y. Wang, *RSC Advances*, 2016, **6**, 93318-93324.
52. A. Mulyadi, Z. Zhang, M. Dutzer, W. Liu and Y. Deng, *Nano Energy*, 2017, **32**, 336-346.
53. Q. Zhao, Q. Ma, F. Pan, Z. Wang, B. Yang, J. Zhang and J. Zhang, *Journal of Solid State Electrochemistry*, 2016, **20**, 1469-1479.
54. Y. Li, H. Zhang, P. Liu, Y. Wang, H. Yang, Y. Li and H. Zhao, *Electrochemistry Communications*, 2015, **51**, 6-10.
55. Q. Liu, Y. Duan, Q. Zhao, F. Pan, B. Zhang and J. Zhang, *Langmuir*, 2014, **30**, 8238-8245.
56. X. Zhang, D. Yu, Y. Zhang, W. Guo, X. Ma and X. He, *RSC Advances*, 2016, **6**, 104183-104192.
57. X. Liu, Y. Zhou, W. Zhou, L. Li, S. Huang and S. Chen, *Nanoscale*, 2015, **7**, 6136-6142.
58. S. Gao, H. Fan and S. Zhang, *Journal of Materials Chemistry A*, 2014, **2**, 18263-18270.
59. L. Zhao, *RSC Advances*, 2017, **7**, 13904-13910.
60. N. K. Chaudhari, M. Y. Song and J.-S. Yu, *Scientific Reports*, 2014, **4**, 5221.
61. I. S. Amiinu, J. Zhang, Z. Kou, X. Liu, O. K. Asare, H. Zhou, K. Cheng, H. Zhang, L. Mai, M. Pan and S. Mu, *ACS Applied Materials & Interfaces*, 2016, **8**, 29408-29418.
62. Y. Lei, L. Wei, S. Zhai, Y. Wang, H. E. Karahan, X. Chen, Z. Zhou, C. Wang, X. Sui and Y. Chen, *Materials Chemistry Frontiers*, 2018, **2**, 102-111.